Investigations of the Dynamic Properties of Matter Using Axis-Symmetrical Shock Waves

Final Subcontractor Report

prepared by

S. N. Dudin, G. I. Kanel, V. B. Mintsev,
S.V. Razorenov, and A. V.Utkin
Russian Academy of Sciences
IVTAN, Izhorskaya
Moscow, Russia

May 1997

IAT.R 0123

Institute for Advanced Technology
The University of Texas at Austin
IAT

REPORT DOCUMENTATION PAGE

Form Approved
OMB NO. 0704-0188

1. AGENCY USE ONLY (Leave blank)	2. REPORT DATE	3. REPORT TYPE AND DATES COVERED

4. TITLE AND SUBTITLE

Investigations of the Dynamic Properties of Matter Using Axis-Symmetrical Shock Waves

5. FUNDING NUMBERS

Contract # DAAA21-93-C-0101

6. AUTHOR(S)

S. N. Dudin, G. I. Kanel, V. B. Mintsev, S.V. Razorenov, and A. V.Utkin

7. PERFORMING ORGANIZATION NAME(S) AND ADDRESS(ES)

Institute for Advanced Technology
The University of Texas at Austin
4030-2 W. Braker Lane, #200
Austin, TX 78759

8. PERFORMING ORGANIZATION REPORT NUMBER

IAT.R 0123

9. SPONSORING / MONITORING AGENCY NAME(S) AND ADDRESS(ES)

U.S. Army Research Laboratory
ATTN: AMSRL-WT-T
Aberdeen Proving Ground, MD 21005-5066

10. SPONSORING / MONITORING AGENCY REPORT NUMBER

11. SUPPLEMENTARY NOTES

The view, opinions and/or findings contained in this report are those of the author(s) and should not be considered as an official Department of the Army position, policy, or decision, unless so designated by other documentation.

12a. DISTRIBUTION / AVAILABILITY STATEMENT

Approved for public release; distribution unlimited.

12b. DISTRIBUTION CODE

A

13. ABSTRACT *(Maximum 200 words)*

The technique for experiments with the cylindrical shock loading of ceramic tube samples has been developed. In experiments, the shock loading of AD998 tubes was realized in two ways: by cylindrical detonation initiated by electrical explosion of wire and by impact of the stainless steel tube liner launched by the cylindrical detonation wave. The Lagrangian computer code for simulations of the shock-wave processes with axial symmetry has been developed and used for interpretation of experimental data. VISAR measurements of the velocity profiles have been carried out with water windows. Results do not correspond to the response of the elastic-plastic body and are the subject of forthcoming analysis.

14. SUBJECT TERMS

Alumina

15. NUMBER OF PAGES

19

16. PRICE CODE

17. SECURITY CLASSIFICATION OF REPORT	18. SECURITY CLASSIFICATION OF THIS PAGE	19. SECURITY CLASSIFICATION OF ABSTRACT	20. LIMITATION OF ABSTRACT
Unclassified	Unclassified	Unclassified	UL

Table of Contents

Preface iii

Introduction 1

Material 2

Measurements 2

Computational Study of Experimental Arrangement 3

Shock-wave generators 5

Study of axis-symmetrical loading of AD998 ceramic tubes 14

Conclusion 19

References 19

Distribution List 20

Table of Figures

Figure 1. Scheme of recording of the free-surface velocity history 3

Figure 2. The structural multi-elements Marzing model (a) 4
and its stress-strain diagram (b).

Figure 3. Streak record of the detonation front 6

Figure 4. The scheme of first version of the launching facility 7

Figure 5. Experimental assembly for experiment with recording the shape of the liner ... 8

Figure 6. Streak records of the impact of copper liners 8

Figure 7. Acceleration of copper tube liners by a cylindrical detonation wave. 9

Figure 8. Shock loading by cylindrical liner 10

Figure 9. Teflon liner 21/28 mm diameter, wire 0.07 mm 10

Figure 10. Impact of the teflon liner upon A1 target. 11

Figure 11. Scheme of the explosive launching facility with an insulated metal liner 11

Figure 12. Streak images of impact of copper (left) and stainless steel (right) 12

Figure 13. Acceleration of copper and stainless steel tube liners 13

Figure 14. Impact of the stainless steel liner upon the aluminum tube target. 14

Figure 15. Results of the VISAR measurements of velocity profiles 15

Figure 16. The particle velocity profiles for ceramic tubes 15

Figure 17. Comparison of measured and calculated velocity profiles 16

Figure 18. Trajectory of the changing state of a middle cylindrical layer of 17
the ceramic tube sample.

Figure 19. Accumulation of a total plastic strain in the middle cylindrical layer 18

Figure 20. Measured and computed VISAR velocity profiles of the AD998 tube 19

Preface

The work described in this report was completed by Gennady Kanel as part of his duties as an IAT Visiting Fellow. The purpose of this project was to develop a new experimental technique that, combined with other work in progress at IAT, can be used to fully characterize the high strain rate behavior of alumina. The work at IAT was coordinated by Dr. Stephan Bless.

HIGH ENERGY DENSITY RESEARCH CENTER
Russian Academy of Sciences
IVTAN, Izhorskaya 13/19, Moscow, 127412 Russia
Telex 411959 IVTAN SU, Telephone (095) 485-79-88, Fax: (095) 485-79-90

INVESTIGATIONS OF THE DYNAMIC PROPERTIES OF MATTER USING AXIS-SYMMETRICAL SHOCK WAVES.

S.N.Dudin, G.I.Kanel, V.B.Mintsev, S.V.Razorenov, A.V.Utkin

Principal investigator: Prof. G.I. Kanel

Introduction

To predict results of an explosion or impact, we need information about the mechanical properties of materials at high pressures, high strain rates and large strains. Experiments with plane shock waves provide an ability to study the mechanical properties of materials under high pressure and extremely high strain rates. For this purpose, well-developed experimental techniques and methods of analyzing the experimental data are at hand of investigators. Measurements of stress or particle velocity histories under shock-wave compression and unloading give information about the dynamic elastic limit, strain rate and way of loading-unloading process in stress-strain coordinates. However, the typical strain values are small in the plane shock waves and increase in the strain is usually connected with an inevitable pressure growth. Meanwhile, in the explosion and high-velocity impact problems, the strain reaches very large values and high pressure takes place usually only during a short wave phase of the process. It would be desirable to expand the possibilities of plane-wave experiments to larger deformations.

New prospects in this regard can be reached by arrangement of the impact loading with cylindrical or spherical symmetry. An additional transverse deformation which is proportional to the radius increment will increase the total strain in this case.

The objective of this work is the development of an experimental method to study the behavior of brittle materials at loading by divergent shock waves. Experimental and theoretical investigations during the last two decades of the response of hard, brittle material (ceramics, glasses and rocks) to shock-wave loading, impact and penetration show a significantly more complicated behavior in comparison with metals and polymers. Deformation of brittle materials is accompanied by failure. The post-failure material response may dominate the total resistance to deformation. A complete description of the inelastic

behavior of brittle materials would contain strain-rate phenomena, post-failure friction of the confined comminuted material, effects of dilatation and its influence on the compressibility and elastic modules. Consequently, models of inelastic behavior of brittle materials need to be rather sophisticated. Numerous parameters of material have to be determined empirically. For this, the stress-strain range has to be expanded beyond the regions accessible in conventional 1-D strain and 1-D stress tests.

Some preliminary measurements of spherical shock waves in alumina were performed by J.-Y. Tranchet (France) and a group from the Stanford Research Institute. The advantage of the spherical symmetry is an additional strain component. Also, experiments with spherical symmetry of detonation, which create a spherical shock wave in the sample, can be easily arranged. The disadvantage of this symmetry is fast decay of the spherical shock wave in the sample. To provide the peak stress above the elastic limit of ceramics, a relatively large explosive charge has to be used. But for small radii, stresses vary so rapidly with position and time that interpretation of data is difficult. On the other hand, for large radius of the explosive charge, a contribution of the spherical symmetry will be rather small. Experimental schemes with cylindrical symmetry suppose more freedom in varying the load parameters and look more promising. Nevertheless, until now cylindrical loading experiments were not involved in investigations of behavior of ceramics under dynamic loading.

Material

The samples for tests were cast AD-99.8 Alumina tubes from the Coors Ceramics Company. The tubes were 1.75" in the outside diameter, 1.5" in the inside diameter, and 4.0" long. The tubes were rather far from ideal cylinders: their diametrical deviations from a circle reached 0.6 mm.

Measurements

Two kinds of measurements were done in this work: fast photo-recording of the process with a streak camera and measurements of the velocity history. The streak camera was used to record a shape of detonation wave or of an impactor and thereby the quality of the load conditions was determined. The streak camera experiments will be described later.

All our experiments were based on initiation of cylindrical detonation by electrical explosion of wires. Since this is accompanied by a very high level of electrical noise, we were not able to use any sensors which have to be placed near to the exploding wire. In this sense, the simplest way to provide measurements is to use a laser Doppler velocimeter. In our work, we used VISAR in a standard configuration [1] with the velocity-per-fringe constant of 305 or 80.8 m/sec. The laser beam of VISAR was directed along the assembly radius as it is shown in Figure 1. We measured the free surface velocity as well as the velocity history of interface with water or LiF window.

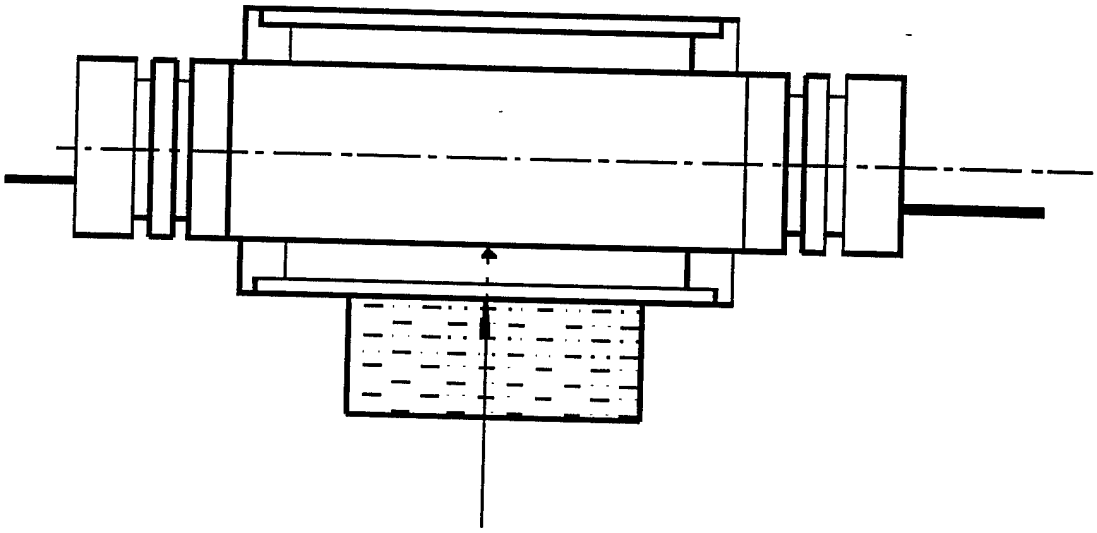

Figure 1. Scheme of recording of the free-surface velocity history or particle velocity history at the interface between the tube sample and LiF or water window. The cylindrical shock wave is created by detonation of an RDX charge initiated by an electrical explosion of a wire on the charge axis.

Computational Study of Experimental Arrangement

1-D Lagrangian code EPIF2 was developed for computer simulation and analysis of experimental data. EPIF2 code uses a simple equation of state of the Mie-Gruneisen type with the cold compression isentrope calculated through the Hugoniot of matter basing on coinciding of the Hugoniots and isentrope in the pressure-particle velocity plane. The Gruneisen parameter is assumed to be constant.

The elastic-plastic properties of materials are described by the structural Marzing model which presents each elementary volume as a series of parallel elastic-viscous-plastic sub-elements [2,3] as shown in Figure 2a and b. This model reflects a micro-nonuniformity of real materials and is successfully used to describe the Baushinger effect at repeated-alternating loading. Sub-elements have equal elastic modules but different yield strength, Y_k, and viscosity. The deviatoric stress in elementary volume is determined as:

$$\sigma = \sum_{k=1}^{N} \sigma_k g_k,$$

where N is the amount of sub-elements, σ_k and g_k are the stress in sub-element and the weight factor.

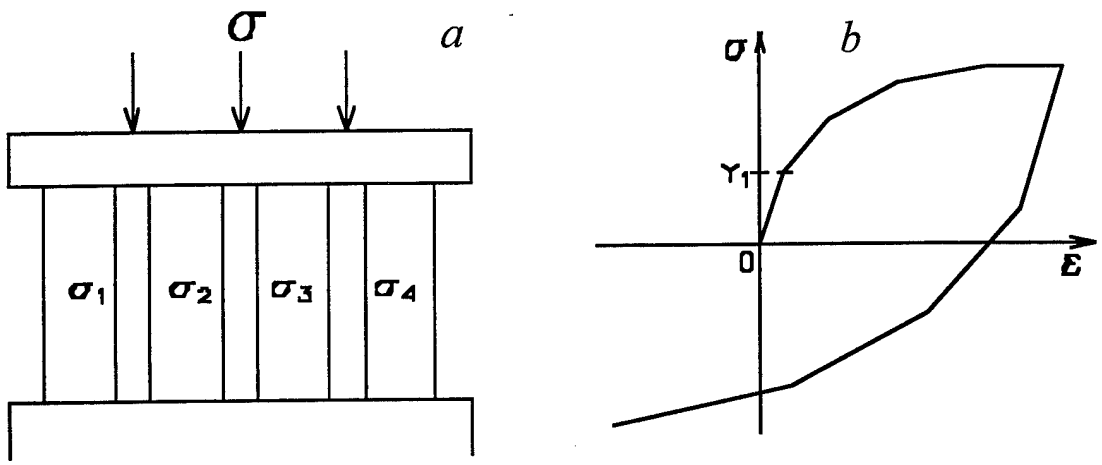

Figure 2. The structural multi-elements Marzing model (a) and its stress-strain diagram (b).

The model includes strain hardening and strain softening of sub-elements:

$$Y_k = Y_{0k} + s_k \gamma_{k,pl}, \quad Y_k \le Y_{k,max}$$

where Y_{0k} is an incident yield stress of the sub-element, s_k is a strain-hardening coefficient of the sub-element, $\gamma_{k,pl}$ is a plastic strain in the sub-element, and $Y_{k,max}$ is an ultimate yield stress. Nonlinear viscosity of the materials is described by the Swegle-Grady relationship [4]:

$$\dot{\gamma}_p = A'(\tau - Y/2)^2.$$

Viscosity of sub-elements is calculated in proportion with yield stress.

All calculations were done with N=2. The yield stress was reducing with development of the fracture.

The code has been constructed to make a computer simulation of cylindrical shock waves created by the liner impact or by a cylindrical detonation wave. In the case of liner impact, initial conditions corresponded to distribution of particle velocity inside the liner as $u=u_{surf} r_{surf}/r$, where r_{surf}, u_{surf} are the liner outside surface radius and velocity. In the case of the detonation wave, the central part of the cylinder assembly was filled with explosive products with a polytropic equation of state $pV^n = const = p_{C\text{-}J} V_{CJ}{}^n$, where $p_{C\text{-}J}$, V_{CJ} are the pressure and specific volume in the Chapman-Jouguet plane, and the exponent $n = U_{det} / (u_{CJ} - 1)$. The initial distributions of pressure, particle velocity and specific volume in the

detonation products roughly corresponded to an approximate solution [5] for the divergent cylindrical detonation wave. It was assumed that a central part of the gas cylinder, about half of its total radius, is under constant pressure and has a zero particle velocity. In the outer part of detonation products, there is a smooth pressure and particle velocity growth to the Chapman-Jouguet state. The initial particle velocity $u_p(r)$ was related to the pressure through the sound velocity:

$$u_p = \frac{2c(p) - U_{\text{det}}}{n-1}.$$

where the sound speed $c = \sqrt{npV}$.

Shock-wave generators

The experimental technique is based on generation of cylindrical divergent shock waves in the tube-like specimens. The axis-symmetrical shock load pulses were created by cylindrical detonation of an explosive charge placed inside the specimen or by impact of cylindrical liners. The liners also were launched by detonation.

In the experiments performed, cylindrical shock waves were created by detonation of the high explosive (HE) which was powder-like RDX of 1.25 g/cm^3 density. Arrangement of the cylindrical detonation wave is a key aspect of the technique. In our experiments, the cylindrical detonation wave was initiated by the electrical explosion of a wire placed along the HE charge axis. For this purpose a standard pulse high-voltage facility VU-19 was used. From discharge of a 0.1 μF capacity bank, this facility generates an electrical pulse of 60 kV voltage and ~1 μsec duration. This electrical pulse was applied to a exploding copper wire 100-120 mm long. The wire diameter was varied from 70 to 120 μ to find the optimum size for initiation of detonation.

To use any facility for measurements as a shock-wave generator, we have to be sure of the shock front symmetry and we have to know the shock wave intensity. When the facility was worked out, the streak camera was used to record the detonation front or a shape of the liner launched by cylindrical detonation. Figure 3 shows a scheme of experiments where initiation of detonation and the detonation front shape were examined. The RDX charge with initiating wire was placed into a rectangular box made of PMMA plates. The streak camera, looking on the target through a narrow slit which is parallel to the wire, records luminosity of the detonation front when it arrives on the PMMA window. The image on the camera film, what we obtain as a result of the experiment, reflects the detonation front shape.

The streak record demonstrates that the exploding wire 70 μ thick provides simultaneous initiating of detonation along at least 100 mm. The central cylindrical part ~80 mm long is large enough. As a result of the edge unloading effect, upper and lower sections of the detonation front come later. The tilt of the central cylindrical part of the detonation front does not exceed 0.3 μsec.

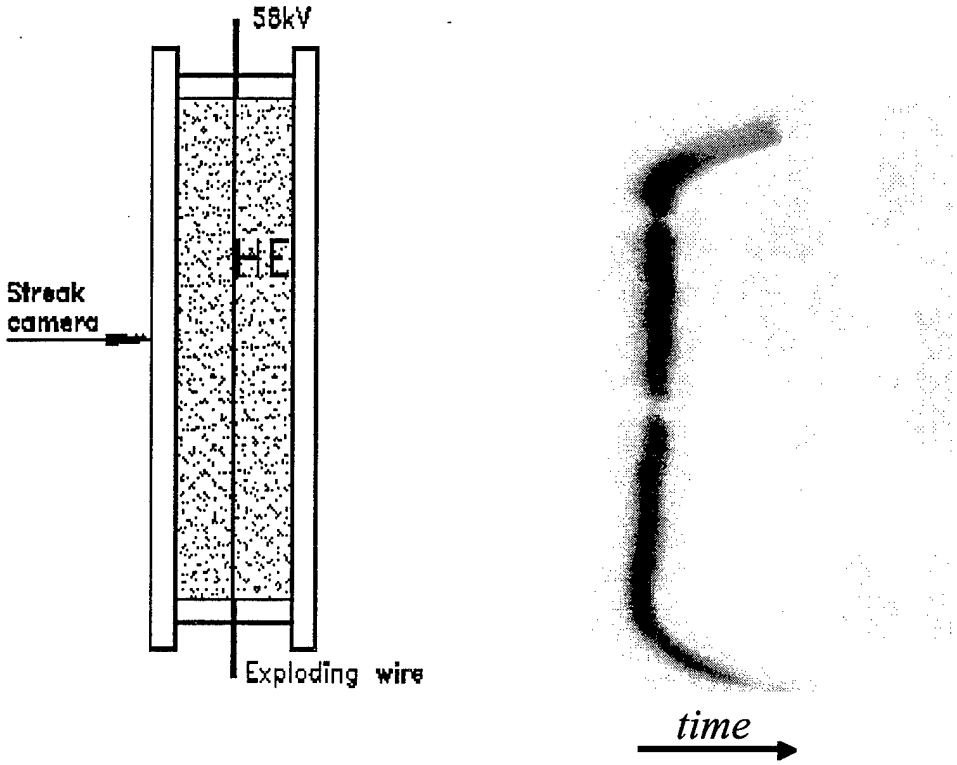

Figure 3. Streak record of the detonation front. The RDX layer is 24 mm thick in total.

Thus, the explosive facility with axial initiation of detonation by electrical explosion of a wire can be, in principle, accepted as a generator of cylindrical shock waves or as a launcher for cylindrical liners. In the case of application of detonation directly as a shock-wave generator, there can be a problem accurately identifying the load conditions since we do not know exactly the shock-to-detonation transition range and the contribution of the chemical spike of the detonation wave. In this sense, the liner should have some advantage as a shock-wave generator.

On the next step, a lot of efforts have been spent to develop a launching facility for tube-like liners. Figure 4 shows the main scheme of the launching facility.

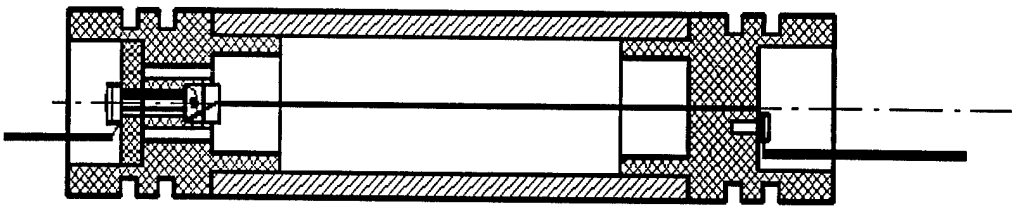

Figure 4. The scheme of first version of the launching facility.

Dimensions of the facility were chosen trying to satisfy two contradictory conditions. The axial dimension of the liner has to provide one-dimensional flow with axial symmetry during whole time of measurements. The gap between the liner and the tube sample, which has to be placed concentrically around the liner, has to be large enough to provide acceleration of the liner by the detonation products and its unloading during the flight. On the other hand, the inside diameter has to be large enough also to provide a reproducible steady detonation wave and some minimum duration of the detonation pressure pulse. The liner wall thickness has to be large enough to provide the shock pulse duration for more than the wave reverberation time in the sample wall. Finally, we worked with liners of 28 to 30 mm in outside diameter, 21 to 24 mm in inside diameter and 100 mm long.

The main problem was insulation of the high-voltage electrical discharge when we used the metal liner. To prevent a break-down between the electrical leads-in and liner, the former were placed into Teflon plugs with large outside surfaces. One of the plugs had several holes through which the liner was filled with the RDX powder. Necessary density and uniformity of the explosive charge was reached by means of vibration of the whole assembly.

Quality of the launching facility was examined by recording the liner shape at the moment when collision with a tube target occurs. This was done using a streak camera by means of the flash-gap method. The scheme of experiments is presented in Figure 5. An assembly of PMMA plates with a gap between them was installed at a distance of 4 mm from the liner surface. The impact of the liner upon the PMMA plates caused adiabatic compression and heat luminosity of a gas inside the gap. The slit of the streak camera was oriented along the assembly axis. The streak record is an image of the luminosity displacement with time when the impact point is shifting along the assembly axis. Thus, the streak record shape reflects the shape of the impacting liner. To increase the luminosity, the gap was filled by argon.

Figure 6 shows examples of the streak records in this series. The pictures demonstrate non-simultaneous impact of the flyers upon the plane target. This means the flyers do not keep their cylindrical shape during acceleration.

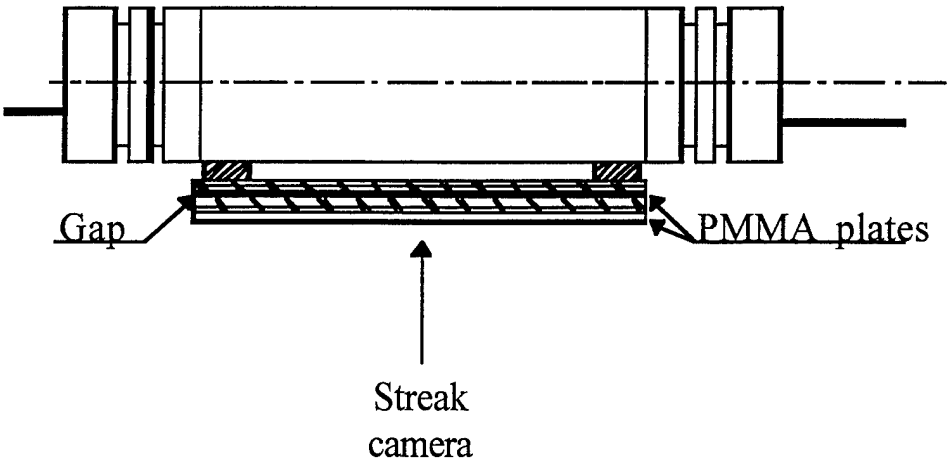

Figure 5. Experimental assembly for experiment with recording the shape of the liner.

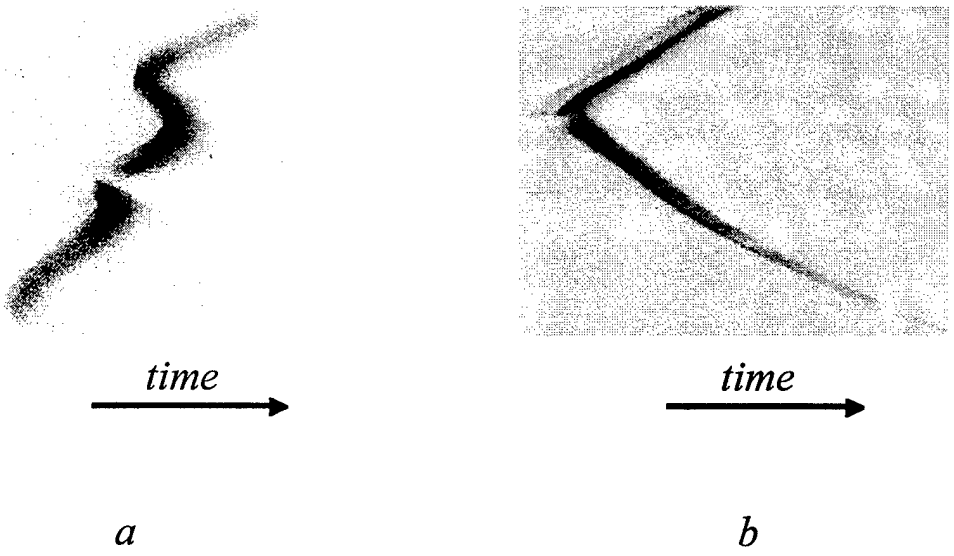

Figure 6. Streak records of the impact of copper liners with a 21 mm inside diameter and a 28 mm outside diameter upon the PMMA assembly.

Additional information on the launching conditions and state of the liner was obtained by recording the velocity of the liner surface. Figure 7 presents these measurements. The liner surface starts to move with low velocity that means there was not a normal detonation wave

yet. General acceleration of the liner is accompanied with oscillations of the velocity which are a result of multiple reverberations of waves inside the liner wall. Velocity profiles are not entirely reproducible: besides different initial jumps, additional velocity jumps appear on different profiles in different time moments. More detailed examination has shown that a reason for these jumps is, obviously, electrical break-down between the exploding wire or leads-in and the metal liner. These accidental discharges destroy the cylindrical detonation wave and initiate additional longitudinal shock waves or detonation waves which propagate along the cylinder axis. Collision of such longitudinal waves produces a specific "bubble" on the liner surface, as indicated in Figure 6a. Passing through a focal spot of the VISAR, such longitudinal waves produce the jumps in the velocity profile.

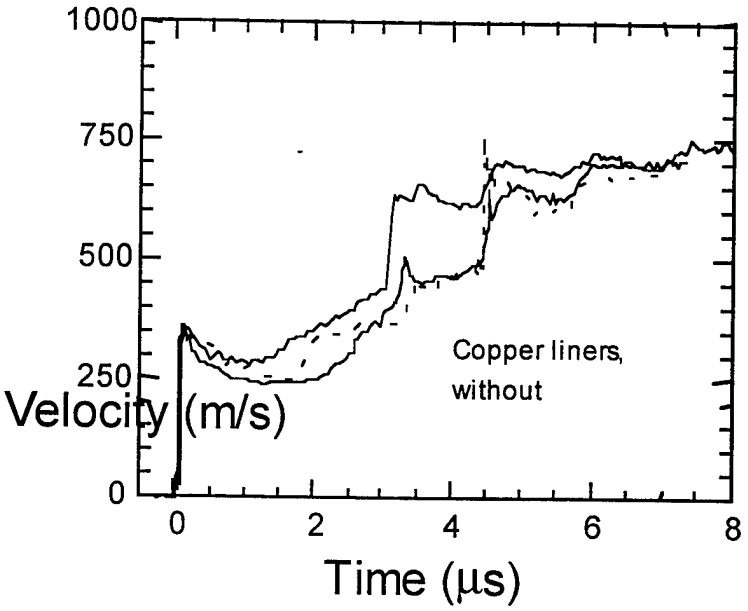

Figure 7. Acceleration of copper tube liners by a cylindrical detonation wave.

Figure 8 shows the results of attempts to record the profile of a stress wave created in the ceramic tube samples by this facility. Measurements were done with a water window. As a result of low quality of the impact conditions and high sound speed in the ceramic, the VISAR velocity profiles demonstrate abnormally large rise time and are certainly distorted. Thus the simple launching facility cannot be used in measurements as a generator of cylindrical shock waves.

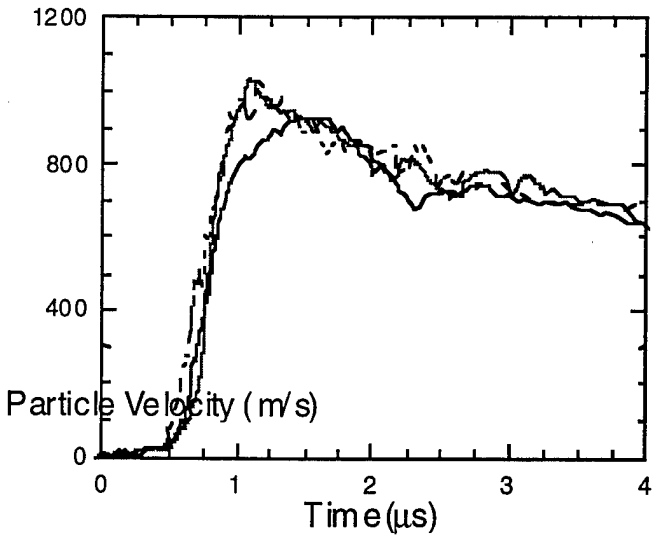

Figure 8. Shock loading by cylindrical liner

Since detonation initiated in a dielectric box has a cylindrical front of good quality, as seen in Figure 3, a reason for distortion of the liner can be only a break-down between the electrical leads-in and metal liner. The break-down takes part of the energy coming to the exploding wire and creates additional points of initiation of detonation.

Generally speaking, the liner can be made of a dielectric material. We investigated this possibility using teflon tubes. Figure 9 presents the streak record of impact of the teflon liner upon the PMMA plate assembly after 4 mm of the flight distance. Indeed, the liner surface distortion is much less in this case. However, the strength of teflon is very small, therefore the spall fracture may occur during launching. Figure 10 shows the VISAR velocity profiles recorded in aluminum tube targets with a water window. Obviously, the teflon liners were failed by the detonation wave.

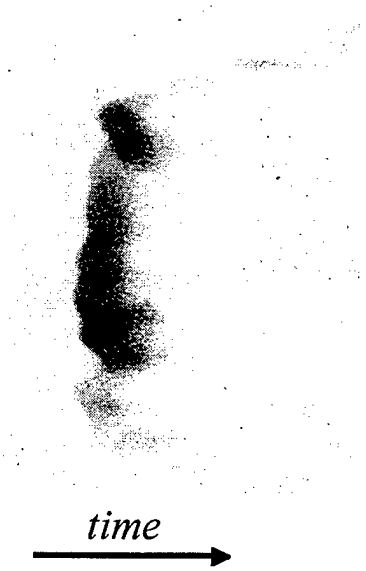

Figure 9. Teflon liner 21/28 mm diameter, wire 0.07 mm

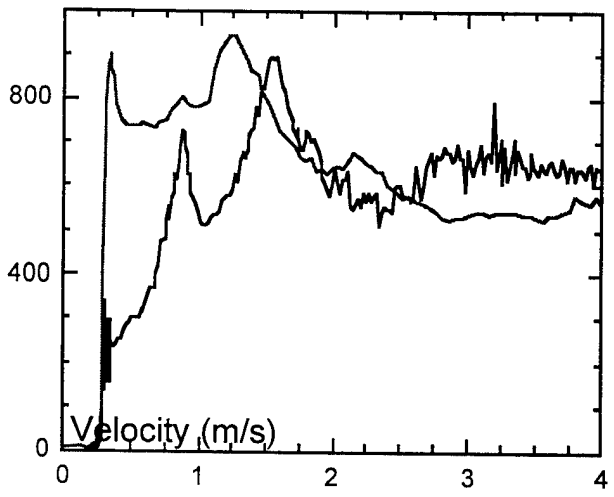

Figure 10. Impact of the teflon liner upon Al target. Measurements with a water window.

Thus, only metal liners can be used in similar facilities, but special efforts have to be undertaken to prevent the electrical break-down. Figure 11 shows a scheme of the next generation of launching facilities. In this facility, the inside surface of a metal liner was additionally insulated by a teflon or PMMA tube with a wall 1 mm thick. A way of possible discharge along the outside surface was essentially increased by means of additional dielectric disks.

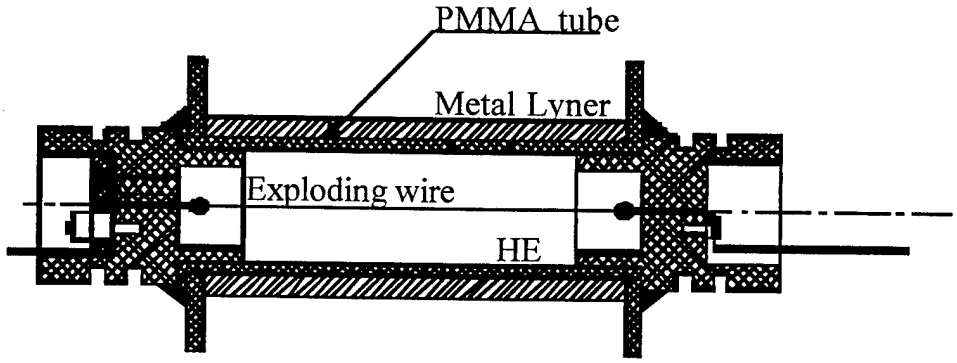

Figure 11. Scheme of the explosive launching facility with an insulated metal liner.

Figure 12 presents the streak camera records of impact of the stainless tube liner launched with this facility upon an assembly of PMMA plates. The additional insulation provides sufficiently good symmetry of impact.

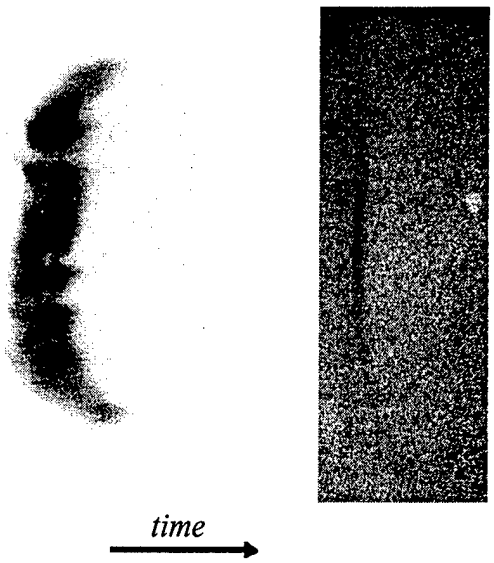

Figure 12. Streak images of impact of copper (left) and stainless steel (right) liners with an outside diameter of 30 mm, inside diameter of 24 mm and a teflon insulator 1 mm thick upon the PMMA plates assembly. The exploding wire is 0.07 mm thick.

Figure 13 presents results of these measurements of velocity of the liner surface for facilities with an insulating insert. The insulating insert removes a way of consumption of the energy of initiating pulse besides the exploding wire. Due to that, the shock-to-detonation transition range becomes shorter and the detonation wave is completely built in this case. As a result, there is higher peak shock pressure and pressure gradient inside the liner wall. Acceleration of the liners becomes more regular. A negative effect in this case is that spall fracture occurs in the liner. We tried to improve the state of the liner by using stainless steel instead of copper because spall strength of the stainless steel is higher than that of copper. We also have changed the teflon insert for the PMMA insert because the teflon has an intermediate dynamic impedance between detonation products and copper or steel and thereby an amplification should occur at transition from HE detonation to shock wave inside the liner. Spalling occurred in this case also, however, due to higher spall strength and a much more viscous fracture. The velocity of the spalled outside layer was less for steel than that for copper. As a result, a residual inner part of the liner during its acceleration by the explosion products overtook the spalled layer and produced a second velocity jump. We hope that, due to this collision, the liner can be re-consolidated and should be able to produce the same shock pulse at impact like a solid liner.

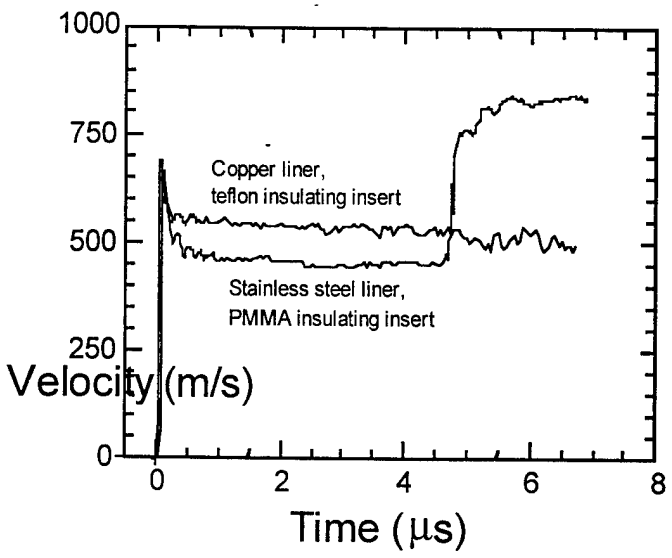

Figure 13. Acceleration of copper and stainless steel tube liners by a cylindrical detonation wave with PMMA or teflon insulating inserts.

Figure 14 shows the result of experiments which were performed with a goal to examine the state of the liner in the time moment of collision with a tube target. In this shot, a VISAR velocity profile of an aluminum tube was recorded through the water window. Experimental data are compared with the result of computer simulation. In principle, the quality of impact is reasonably good, but the duration of measured shock pulse is somewhat more than that in the calculated profile. This means that complete consolidation of the liner probably did not occur. We did not estimate reproducibility of the liner state and impact. Perhaps, disagreement in the stress pulse amplitude is a result of scatter in the launching conditions. On the other hand, it is necessary to consider in more detail the state of the liner in the impact moment. In calculations, we assumed that the liner is absolutely free in the impact moment. However, since it is an expanding tube, there have to be hoop stresses on the yield limit inside the liner. The response of such stressed material at impact has to be analyzed specifically. A state and contribution of the PMMA lye behind the liner are not quite clear either.

Thus, after much effort we have to conclude that normal detonation waves produce irreversible damage to tube liners which make difficult an interpretation of experimental data obtained with such a facility. Nevertheless, after some calibration, such a facility can be used for measurements such as the shock-wave generators with cylindrical symmetry.

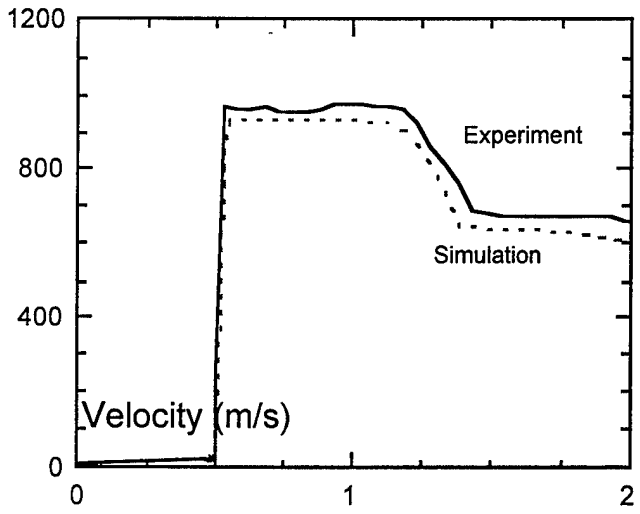

Figure 14. Impact of the stainless steel liner upon the aluminum tube target. The liner is 24 mm in the incident inside diameter and 30 mm in outside diameter. The target is 42 mm in outside diameter and 37 mm in inside diameter. The velocity of the target surface is measured with a water window.

Study of axis-symmetrical loading of AD998 ceramic tubes

Figure 1 shows the scheme of experiments with measurements of the velocity history of the tube sample surface with cylindrical detonation as a shock-wave generator. Measurements were done with ceramic and PMMA tubes using water or LiF windows. The windows had to provide support for some finite pressure during the time of measurement. The shot with PMMA was done as a test shot with a goal to verify the load conditions. The PMMA tube had an inside diameter of 37 mm and an outside diameter of 43 mm. The AD998 ceramic tubes were 36.9±0.3 mm in inside diameter and 43.15±0.2 mm in outside diameter.

The velocity histories of interfaces between the tube samples and water window are presented in Figure 15. Figure 16 compares velocity profiles obtained with water and LiF windows. For measurements, aluminum foil 7 μ thick was glued on the sample surface as a reflector for a laser beam from the VISAR. The rest of the surface of the tube samples was also closed by black paper to shield VISAR from luminosity of the detonation. The LiF window was made from a single crystal block. Unfortunately, we were not able to provide good quality VISAR interferograms in shots with LiF windows.

Let us consider more detailed experiments with water windows. In the *p-u* plane, the Hugoniot of PMMA is disposed between the Chapman-Jouguet point and isentrope of the

detonation products which are above and the Hugoniot of water which is below the PMMA Hugoniot. The difference between them is not large. Due to that, the wave reverberations inside the PMMA wall almost are not visible in the velocity profile. Alumina has a much higher dynamic impedance. Oscillations in the velocity profile are the result of multiple wave reverberations inside the alumina wall between the water and detonation products. Finally, since the thickness of alumina is small in comparison with water and detonation products' layers thickness, the same particle velocity is established for the PMMA and alumina in the latter time.

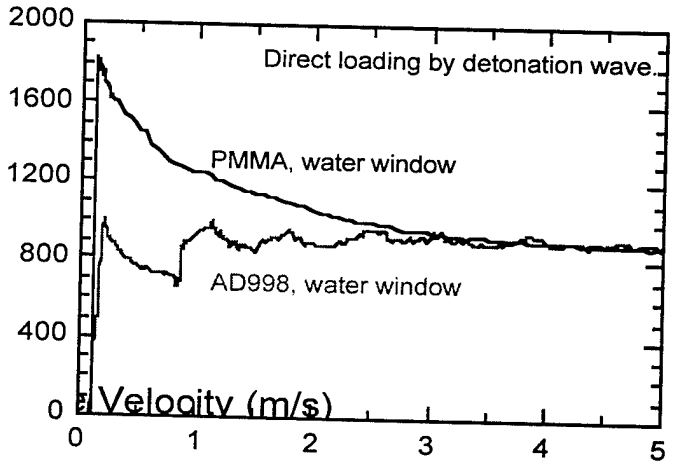

Figure 15. Results of the VISAR measurements of velocity profiles of tube PMMA and AD998 samples with water window.

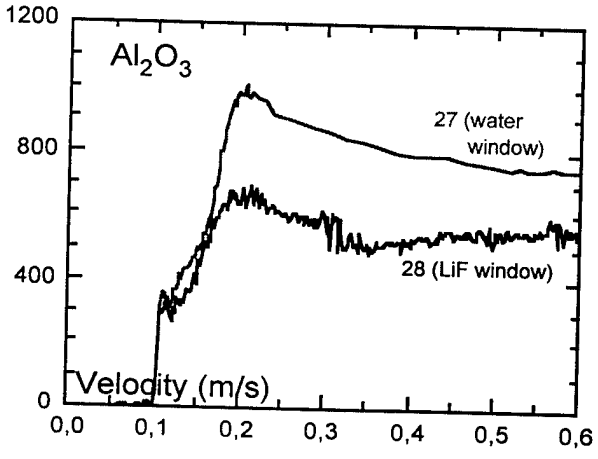

Figure 16. The particle velocity profiles for ceramic tubes at different window materials.

Since the amplitude of oscillations is less than the Hugoniot elastic limit, for an elastic-plastic body it is natural to expect that the oscillations period Δt should be determined by the longitudinal sound velocity c_l: $\Delta t = h / c_l$. Estimations show that measured period essentially exceeds this value and rather corresponds to the bulk sound velocity.

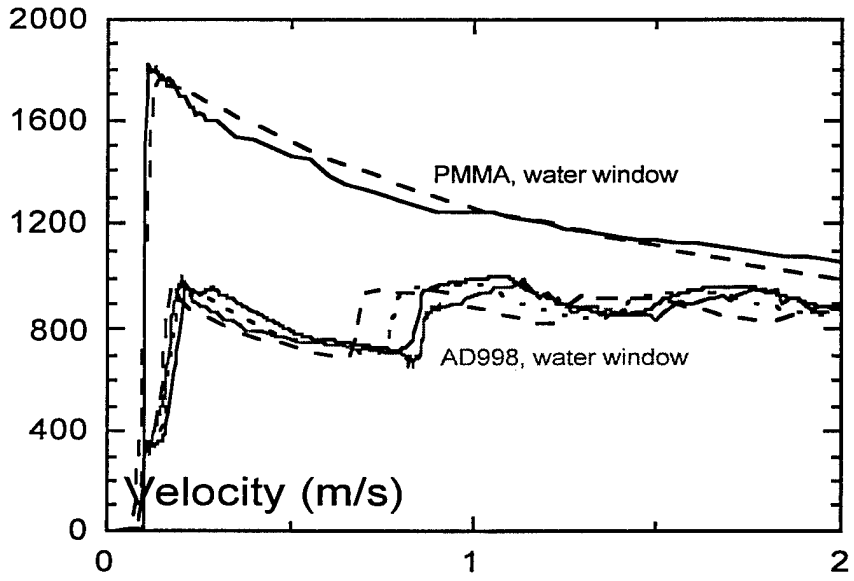

Figure 17. Comparison of measured and calculated velocity profiles of shock waves created in the PMMA and AD998 tube samples by cylindrical detonation. Measurements with water windows.

In the Figure 17, measured velocity profiles are compared with the results of computer simulation. In the first step, the experiment with PMMA was simulated to make a reasonable estimation of the initial distribution of pressure and particle velocity in the detonation products. Since, as it was mentioned above, we used an approximation which did not account for the shock-to-detonation transition range and chemical spike of the steady detonation wave, we have not received a solution which would absolutely coincide with the experimental data. Nevertheless, as a first approximation, there is quite a reasonable agreement for the shot with PMMA. In the next step, a series of simulations has been performed for AD998 using the same initial state distribution of detonation products, which has been estimated from the shot with the PMMA tube. In this series, the same values of the incident yield stress in sub-elements of the Marzing model Y_{01} =5 GPa and Y_{02} =6 GPa were used, but the strain hardening (or softening) was varied. For the equation of state, properties of AD999 (density 3.948g/cm^3, longitudinal sound velocity 10.85 km/sec and

Hugoniot in form of U_s=7.97+1.27u_p) were used as a base. Comparison with the experimental profile shows that there is a good agreement in period of the velocity oscillations when almost complete softening occurs. On the other hand, the initial parts of the unloading wave coincide better when there is not essential softening. It seems the strain softening really takes place, but occurs at low pressure only.

Other results of the computer simulation with softening are presented in Figures 18 and 19 which show a phase trajectory of the changing state of a middle cylindrical layer of the ceramic tube sample during the whole cycle of impact loading and accumulation of a total plastic strain in this layer. Figure 19 demonstrates that the total plastic strain at axis-symmetrical shock loading is much more than that at plane shock loading. In our experiment, the plastic strain reached 15% during 2 μsec of loading by the detonation.

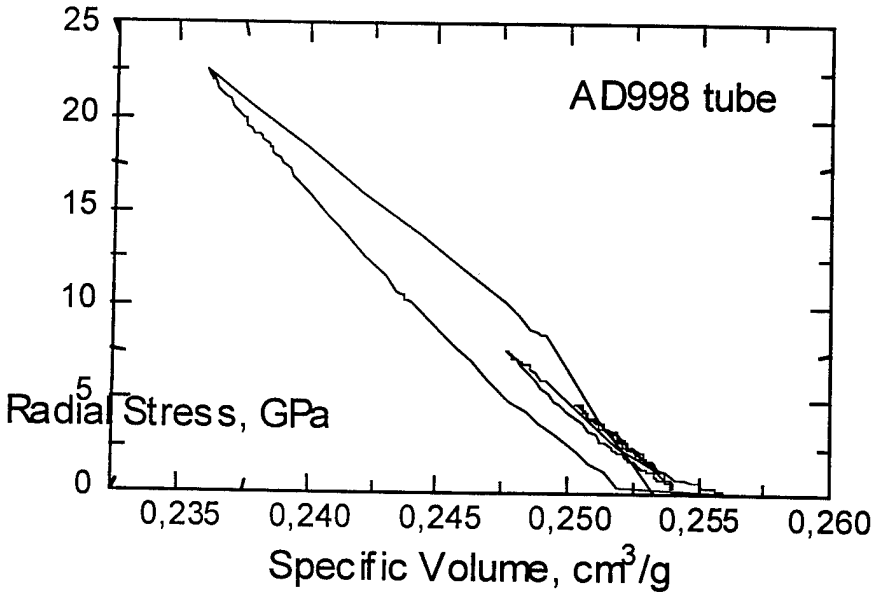

Figure 18. Trajectory of the changing state of a middle cylindrical layer of the ceramic tube sample. Results of computer simulation with large strain softening.

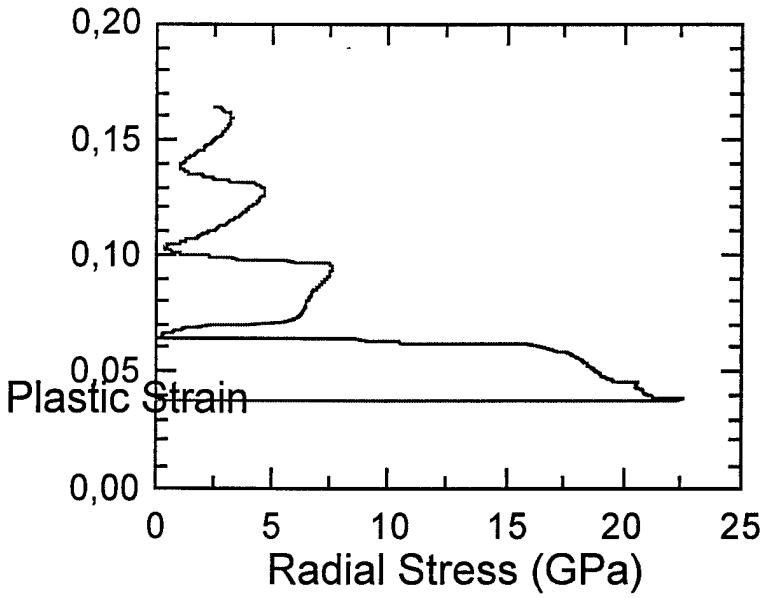

Figure 19. Accumulation of a total plastic strain in the middle cylindrical layer of a ceramic tube sample during 2.5 μsec of cylindrical shock loading.

Figure 20 shows the result of the impact experiment with an AD998 tube sample. Measurements were done with a water window; experiments with the LiF window, again, were not successful. Unlike similar shots with aluminum targets, there is a sloped top of the wave profile recorded. The pulse duration is determined by the impactor thickness and is not so sensitive to properties of the ceramic target. In Figure 20, the measured profile is compared with results of computer simulation without and with softening. The results are not very sensitive to properties of the target material.

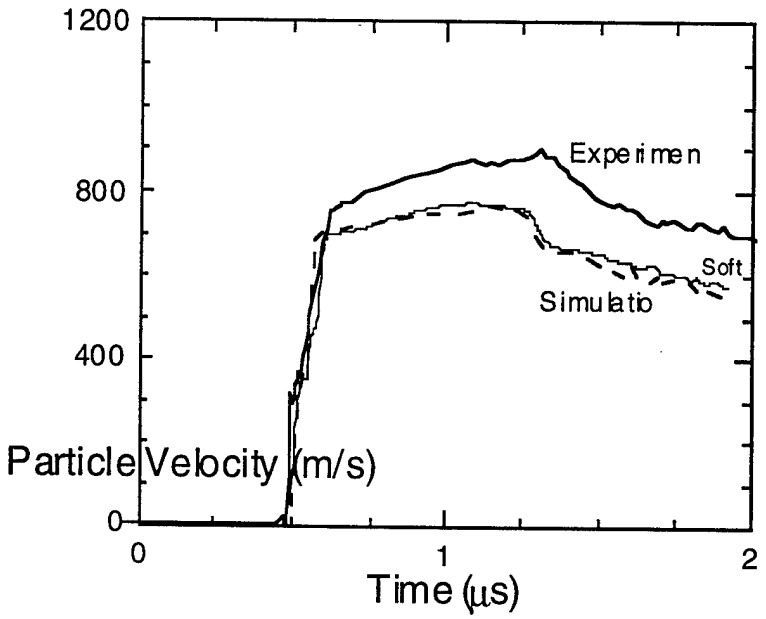

Figure 20. Measured and computed VISAR velocity profiles of the AD998 tube sample impacted by the stainless tube liner. Measurements with a water window.

Conclusion

The technique for experiments with the cylindrical shock loading of ceramic tube samples has been developed. In experiments, the shock loading of AD998 tubes was realized in two ways: by cylindrical detonation initiated by electrical explosion of wire and by impact of the stainless steel tube liner launched by the cylindrical detonation wave. The Lagrangian computer code for simulations of the shock-wave processes with axial symmetry has been developed and used for interpretation of experimental data. VISAR measurements of the velocity profiles have been carried out with water windows. Results do not correspond to the response of the elastic-plastic body and are the subject of forthcoming analysis.

References

[1] J.R. Asay and L. M. Barker, *J. Appl. Phys.*, **45**, 2540 (1974).

[2] D.A.Gokhfeld and O.S. Sadakov. *Plasticity of Structural Elements under Repeated Loads*. (in Russian). Mashinostroenie, Moscow, 1984.

[3] G.I. Kanel. *Problems of Strength (USSR)*, 1988, No 9, p. 55.

[4] J.W. Swegle, D.E.Grady. - *J.Appl. Phys.*, 1985, vol.58, No.2, p.692.

[5] K.P. Stanyukovitch. *Unsteady motions of continuous media (in Russian)*. Nauka, Moscow, 1971.

Distribution List

Administrator
Defense Technical Information Center
Attn: DTIC-DDA
8725 John J. Kingman Road,
Ste 0944
Ft. Belvoir, VA 22060-6218

Director
US Army Research Lab
ATTN: AMSRL OP SD TA
2800 Powder Mill Road
Adelphi, MD 20783-1145

Director
US Army Research Lab
ATTN: AMSRL OP SD TL
2800 Powder Mill Road
Adelphi, MD 20783-1145

Director
US Army Research Lab
ATTN: AMSRL OP SD TP
2800 Powder Mill Road
Adelphi, MD 20783-1145

Army Research Laboratory
AMSRL-CI-LP
Technical Library 305
Aberdeen Prvg Grd, MD 21005-5066

Dr. Charles Anderson, Jr.
Southwest Research Institute
Engineering Dynamics Department
P.O. Box 28510
San Antonio, TX 78228-0510

N. Singh Brar
University of Dayton Research Institute
300 College Park
Shroyer Park Center
Dayton, OH 45469-0182

Rodney J. Clifton
Brown University
Providence, RI 02912

Dr. Datta Dandekar
Army Research Laboratory
AMSRL-MA-PD
Aberdeen PG, MD 21005-5066

William deRosset
U.S. Army Research Laboratory
Attn: AMSRL-WT-TC
Aberdeen Prvg Grd, MD 21005-5066

William A. Gooch
US Army Research Lab
ATTN: AMSRL-WT-TA
Aberdeen Prvg Grd, MD 21005-5066

Tim Holmquist
Alliant Techsystems, Inc.
Twin City Army Ammunition Plant-Bldg. 103
New Brighton, MN 55112

Kailasam Iyer
US Army Research Office
P.O. Box 1221
Research Triangle Park, NC 27709-2211

Gennady Kanel
Institute for High Temperatures
Moscow
Russia 127912

Nick Lynch
DERA Fort Halstead
Bldg. A 20, Div. WX5
Sevenoaks, Kent
England TN14 7BP

Mr. Dennis L. Orphal
International Research Associates
4450 Black Ave. Suite E
Pleasanton, CA 94566

Yehuda Partom
Rafael Ballistics Center
Box 2250
Haifa 31021
Israel

Dr. A. M. Rajendran
US Army Research Lab
AMSRL-MA-PD
Aberdeen PG, MD 21005-5066

Edward Rapacki
Director
U.S. Army Research Laboratory
Attn: AMSRL-WT-TA
Aberdeen Prvg Grd, MD 21005-5066

Dr. Roy Reichenbach
European Research Office
USA RDSG-UK
PSC 802 Box 15
FPO AE 09499-1500

Donald A. Shockey
SRI International
333 Ravenswood Ave
Menlo Park, CA 94025

Distribution List

Dr. Joseph Sternberg
Physics Dept.
Naval Postgraduate School
Monterey, CA 93943

J.Y. Tranchet
Centre d'Etudes Gramat
46500 Gramat
France

Mike Zoltoski
U.S. Army Research Laboratory
Attn: AMSRL-WM-TA
Aberdeen Prvg Grd, MD 21005-5066